Inorganic Chemistry

Article

pubs.acs.org/IC

Dicopper(II) Metallacyclophanes with Oligo(*p*-phenylene-ethynylene) Spacers: Experimental Foundations and Theoretical Predictions on Potential Molecular Magnetic Wires

María Castellano,[†] Francisco R. Fortea-Pérez,[†] Abdeslem Bentama,[†,⊥] Salah-Eddine Stiriba,[†] Miguel Julve,[†] Francesc Lloret,*[,†] Giovanni De Munno,[§] Donatella Armentano,*[,§] Yangling Li,[∥] Rafael Ruiz-García,[†,‡] and Joan Cano*[,†,‡]

[†]Institut de Ciència Molecular (ICMol) and [‡]Fundació General de la Universitat de València (FGUV), Universitat de València, 46980 Paterna, València, Spain

[§]Centro di Eccellenza CEMIF.CAL, Dipartimento di Chimica, Università della Calabria, 87030 Cosenza, Italy

[∥]Institut Parisien de Chimie Moléculaire, CNRS, UMR 7201, UPMC Univ Paris 06, 75252 Paris, France

Supporting Information

ABSTRACT: Two novel double-stranded dicopper(II) metallacyclophanes of formula $(n\mathrm{Bu_4N})_4[\mathrm{Cu_2(dpeba)_2}]\cdot 4\mathrm{MeOH}\cdot 2\mathrm{Et_2O}$ (**1**) and $(n\mathrm{Bu_4N})_4[\mathrm{Cu_2(tpeba)_2}]\cdot 12\mathrm{H_2O}$ (**2**) have been prepared by the Cu^{II}-mediated self-assembly of the rigid ('rod-like') bridging ligands *N*,*N*′-4,4′-diphenylethynebis(oxamate) (dpeba) and *N*,*N*′-1,4-di(4-phenylethynyl)-phenylenebis(oxamate) (tpeba), respectively. Single crystal X-ray diffraction analysis of **1** confirms the presence of a dicopper(II)tetraaza[3.3]4,4′-diphenylethynophane metallacyclic structure featuring a very long intermetallic distance between the two square planar Cu^{II} ions [r = 14.95(1) Å]. The overall parallel-displaced π-stacked conformation of the two nearly planar para substituted diphenylethyne spacers [dihedral angle (ψ) of 7.8(1)°] leads to important deviations from the perpendicular orientation of the copper mean basal planes with respect to the facing benzene planes [dihedral angles (ϕ) of 56.4(1) and 58.4(1)°]. X-band EPR spectra together with variable-temperature magnetic susceptibility and variable-field magnetization measurements of **1** and **2**, both in solution and in the solid state, show the occurrence of a non-negligible, moderate to weak intramolecular antiferromagnetic coupling [$-J$ = 3.9−4.1 (**1**) and 0.5−0.9 cm^{-1} (**2**); $\mathbf{H} = -J\,\mathbf{S_1}\cdot\mathbf{S_2}$ with $S_1 = S_2 = S_{Cu} = 1/2$]. Density functional calculations on the BS singlet (S = 0) and triplet (S = 1) spin states of the model complexes **1** and **2** with an ideal orthogonal molecular geometry (ψ = 0° and ϕ = 90°) support the occurrence of a spin polarization mechanism for the propagation of the exchange interaction between the two unpaired electrons occupying the d_{xy} orbital of each square planar Cu^{II} ion through the predominantly π-type orbital pathway of the double *p*-diphenylethyne (**1**) and di(phenylethynyl)phenylene spacers (**2**). Time-dependent density functional calculations reproduce the observed bathochromic shift of the main intraligand (IL) π−π^* transition in the electronic absorption spectra of **1** and **2** [λ_1 = 308 (**1**) and 316 nm (**2**)]. In the series of orthogonal model complexes **1**−**5** with linear oligo(*p*-phenylene-ethynylene) (OPE) spacers, $-C_6H_4(C{\equiv}CC_6H_4)_n-$ (n = 1−5), a linear increase of the IL π−π^* transition energy with the reciprocal of the intermetallic distance is theoretically predicted [$\nu_{max} = 1.99\times10^4 + 2.15\times10^5\,(1/r)$ (S = 0) or $\nu = 2.01\times10^4 + 2.18\times10^5\,(1/r)$ (S = 1)], which clearly indicates that the effective π-conjugation length increases with the number of phenylethyne repeating units. This is accompanied by an exponential decay of the antiferromagnetic coupling with the intermetallic distance [$-J = 1.08\times10^3\exp(-0.31r)$], which supports the ability of the extended π-conjugated OPEs to mediate the exchange interaction between the unpaired electrons of the two Cu^{II} centers with intermetallic distances in the range of 1.5−4.3 nm. Further developments may be then envisaged for this new family of oxamato-based dicopper(II) oligo-*p*-phenylethynophanes on the basis of the unique ligand capacity to act as a molecular antiferromagnetic wire.

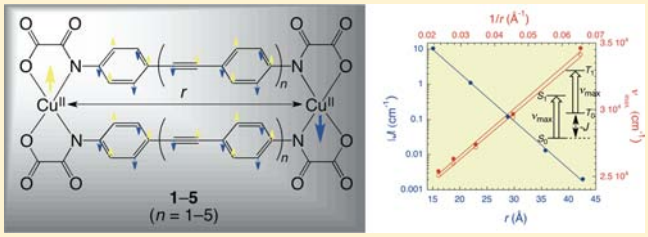

INTRODUCTION

Dinuclear complexes with strong intramolecular electronic interactions between distant metal centers across extended bridges are a common topic in molecular magnetism and molecular electronics.[1] Besides their interest as models for the fundamental research on long-distance electron exchange (EE) and electron transfer (ET) phenomena,[2,3] they are also of great importance in the "bottom-up" approach to nanometer-scale electronic devices such as molecular wires and switches.[4] Molecular magnetic wires may offer a new design concept for the transfer of information over long distances based on purely

Received: March 27, 2013
Published: June 18, 2013

   dx.doi.org/10.1021/ic400754m | *Inorg. Chem.* 2013, 52, 7645−7657

EE (Coulombic) interactions and without any current flow,[5] by comparison with conventional molecular electronic wires which are based on ET interactions instead.[6] However, the examples of long-range magnetic coupling in exchange-coupled dinuclear complexes are relatively scarce with regard to the more abundant examples of long-range electron transport in mixed-valent ones.[7] The design and synthesis of novel bridging ligands which can transmit spin coupling effects over long distances are then a major goal in the field, which require both a skillful organic synthesis and a deep understanding of the EE mechanism.[2c] With the advent of ground- and excited-state calculations based on the density functional (DF) and time-dependent density functional (TD-DF) theory combined with the broken-symmetry (BS) approach, it has been possible not only to reproduce but also to predict very accurately the electronic and magnetic properties of simple dinuclear complexes.[8]

Dicopper(II) metallacyclophanes emerge as ideal model systems for the study of the transmission of EE interactions between paramagnetic metal centers containing one unpaired electron ($\mathbf{H} = -J\ \mathbf{S_1}\cdot\mathbf{S_2}$ with $S_1 = S_2 = S_{Cu} = 1/2$) through potential molecular magnetic wires, both from experimental and theoretical viewpoints.[9] The variation of the ligand spacer in the metallacyclic entity may control the overall structure and the magnetic properties and then, the influence of different factors such as the topology and conformation of the bridging ligand can be investigated in a systematic way.[10−13] So, the problem of long-range magnetic coupling in dicopper(II) metallacyclophanes have been addressed by several research teams through the use of different coordinating group substituted amine-,[10] imine-,[11] and amide-based[12] aromatic bridging ligands, with more or less satisfactory results.

Our strategy in this field involves a unique family of double-stranded dicopper(II) metallacyclophanes resulting from the side-by-side coordination of extended π-conjugated aromatic bis(oxamato) bridging ligands to square planar metal ions (Scheme 1).[13] This type of rigid dinucleating ligands with oligo(*p*-phenylene) (OP) (a of Scheme 1)[13b] and oligo(α,α'- or β,β'-acene) (OA) spacers (b and c of Scheme 1)[13c] are very appealing candidates as molecular magnetic wires. Thus, the oxamato-based dicopper(II) metallacyclophanes with 1,4-phenylene and 4,4′-diphenylene spacers (a of Scheme 1 with $n = 1$ and 2) exhibit a strong to moderate antiferromagnetic coupling ($-J$ values in the range of 81−95 cm^{-1} and 8.7−11.5 cm^{-1}, respectively) at relatively large intermetallic distances (r = 7.9 and 12.2 Å, respectively).[13b] Yet the related pair of oxamato-based dicopper(II) metallacyclophanes with 1,5-naphthalene and 2,6-anthracene spacers (b and c of Scheme 1 with $n = 2$ and 3, respectively) show a similar moderate antiferromagnetic coupling ($-J$ values in the range of 20.5−20.7 cm^{-1} and of 21.2−23.9 cm^{-1}, respectively) in spite of the largely different intermetallic distances (r = 8.3 and 12.5 Å, respectively).[13c,f] More importantly, DF calculations on these two series of oxamato-based dicopper(II) metallacyclophanes with OA spacers predict a unprecedented wire-like magnetic behavior for the longer members of the series with octacene through decacene spacers (b and c of Scheme 1 with n = 8−10).[13c]

These promising results have oriented our current research toward other oxamato-based dicopper(II) metallacyclophanes with linear oligo(*p*-phenylene-ethynylene) (OPE) spacers (d of Scheme 1), as reported in a preliminary communication.[13e] In fact, the rigid rod-like OPE spacers have a potential extended π-conjugation that would allow a non-negligible electronic as well as magnetic coupling between very distant metal centers in both organometallic and coordination compounds.[14,15] Herein we report on the complete synthesis, general physical and/or structural characterization, spectroscopic and magnetic properties of two new examples of oxamato-based dicopper(II) metallacyclophanes of formula $(n\mathrm{Bu_4N})_4[\mathrm{Cu_2(dpeba)_2}]\cdot 4\mathrm{MeOH}\cdot 2\mathrm{Et_2O}$ (**1**) and $(n\mathrm{Bu_4N})_4[\mathrm{Cu_2(tpeba)_2}]\cdot 12\mathrm{H_2O}$ (**2**) [$n\mathrm{Bu_4N^+}$ = tetra-*n*-butylammonium, $\mathrm{H_4}$dpeba = *N*,*N*′-4,4′-diphenylethynebis(oxamic acid), and $\mathrm{H_4}$tpeba = *N*,*N*′-1,4-di(4-phenylethynyl)phenylenebis(oxamic acid)]. Complexes **1** and **2** can be considered as the first two members of a novel series of oxamato-based dicopper(II) metallacyclophanes with OPE spacers of different length, $-\mathrm{C_6H_4(C{\equiv}CC_6H_4)}_n-$ (**1**−**5**, n = 1−5) (d of Scheme 1). DF and TD-DF calculations on the electronic structure of the ground and excited states of the model complexes **1**−**5** have been carried out in order to analyze the effect of the increase of the conjugation length with the number of phenylethyne units in the OPE spacer on both the magnetic coupling and the electronic spectra of this unique series of dinuclear copper(II) complexes with intermetallic distances varying in the range of 1.5−4.3 nm.

Scheme 1. Oxamato-Based Dicopper(II) Metallacyclophanes with Oligo(*p*-phenylene) (a), Oligo(α,α'-acene) (b), Oligo(β,β'-acene) (c), and Oligo(*p*-phenylene-ethynylene) (d) Spacers As Molecular Magnetic Wires

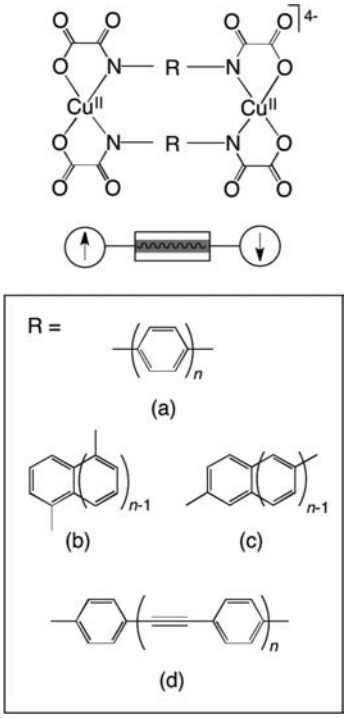

RESULTS AND DISCUSSION

Synthesis of the Ligands and Complexes. The *N*,*N*′-4,4′-diphenylethynebis(oxamic acid) ($\mathrm{H_4}$dpeba) and *N*,*N*′-1,4-di(4-phenylethynyl)phenylenebis(oxamic acid) ($\mathrm{H_4}$tpeba) ligands were prepared through two consecutive steps from the Pd/Cu catalyzed, Sonogashira-type cross-coupling reaction of *p*-ethynylaniline and *p*-iodoaniline or *p*-diiodophenylene respectively,[15a] followed by the straightforward condensation of the resulting 4,4′-diphenylethyne- and 1,4-di(4-phenylethynyl)phenylenediamine precursors with ethyl oxalyl

dx.doi.org/10.1021/ic400754m | Inorg. Chem. 2013, 52, 7645−7657

chloride ester (1:2 molar ratio) in the presence of triethylamine in THF (Scheme 2). They were isolated as the *N*,*N*′-4,4′-diphenylethynebis(oxamic acid ethyl ester) (Et_2H_2dpeba) and *N*,*N*′-1,4-di(4-phenylethynyl)phenylenebis(oxamic acid ethyl ester) (Et_2H_2tpeba) derivatives in good yields (~80−85%, see Experimental Section).

Scheme 2. Synthesis of the Diethyl Ester Derivatives of the H_4dpeba and H_4tpeba Ligands[a]

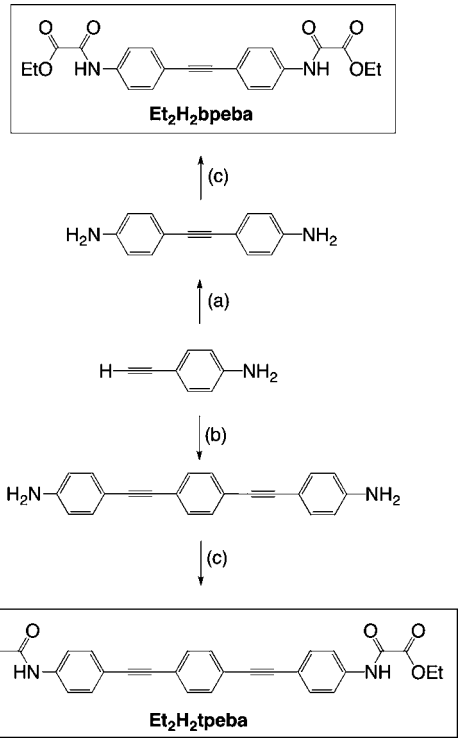

[a]Reaction conditions: (a) *p*-$IC_6H_4NH_2$, $PdCl_2(PPh_3)_2$/CuI, NEt_3; (b) *p*-$C_6H_4I_2$, $PdCl_2(PPh_3)_2$/CuI, NEt_3; (c) C_2O_3EtCl, NEt_3, THF.

Complexes **1** and **2** were then prepared by the reaction of the Et_2H_2dpeba and Et_2H_2tpeba proligands with copper(II) perchlorate hexahydrate (1:1 molar ratio) using nBu_4NOH as base in methanol, and they were isolated as their tetra-*n*-butylammonium salts in good yields (~65−70%, see Experimental Section). X-ray quality dark green prims of **1** were obtained by diethyl ether layering on the methanol solution. Unfortunately, all our attempts to grow X-ray quality crystals of **2** were unsuccessful. The chemical identity of the ligand and complexes was established by elemental analyses and ^{1}H NMR and FT−IR spectroscopies (see Experimental Section). The structure of **1** was further confirmed by single-crystal X-ray diffraction. A summary of the crystallographic data of **1** is given in Table 1, while selected bond distances and angles are listed in Table 2.

Description of the Structure. The structure of **1** consists of centrosymmetric dicopper(II) complex anions, $[Cu^{II}_2(dpeba)_2]^{4-}$, and tetra-*n*-butylammonium cations, together with methanol and diethyl ether as crystallization molecules (Figure 1 and Figure S1, Supporting Information [SI]). In the crystal lattice, the discrete anionic dicopper(II) complexes establish weak hydrogen bonds with the methanol molecules through the carboxylate- and carbonyl-oxygen atoms from the oxamato groups [O(5)···O(8) = 2.760(4) Å and O(6)···O(9) = 2.804(4) Å] (Figure S1a, SI). Yet they are well separated from each other by the bulky tetra-*n*-butylammonium cations and the diethyl ether molecules (Figure S1b, SI). The intramolecular Cu(1)−Cu(1)^{I} distance (*r*) across the double para substituted diphenylethynediamidate bridge is 14.95(1) Å, while the shortest intermolecular Cu(1)−Cu(1)^{II} separation is 8.09(1) Å [symmetry code: (I) = 2 − *x*, 1 − *y*, 2 − *z*; (II) = 1 − *x*, 1 − *y*, 1 − *z*].

Table 1. Summary of Crystallographic Data for 1

formula	$C_{112}H_{196}Cu_2N_8O_{18}$
M (g mol^{-1})	2069.85
crystal system	monoclinic
space group	$P2_1/c$
a (Å)	15.261(2)
b (Å)	25.691(4)
c (Å)	17.279(3)
β (deg)	116.180(6)
V (Å^3)	6079.4(16)
Z	2
ρ_{calc} (g cm^{-3})	1.131
μ (mm^{-1})	0.412
T (K)	100(2)
reflect. collected	10675
reflect. obs. [$I > 2\sigma(I)$]	9467
data/restraints/parameters	10675/0/645
R_1[a] [$I > 2\sigma(I)$] (all)	0.0740 (0.0836)
wR_2[b] [$I > 2\sigma(I)$] (all)	0.2073 (0.2220)
S[c]	1.175

[a]$R_1 = \sum(|F_o| - |F_c|)/\sum|F_o|$. [b]$wR_2 = [\sum w(F_o^2 - F_c^2)^2/\sum w(F_o^2)^2]^{1/2}$. [c]$S = [\sum w(|F_o| - |F_c|)^2/(N_o - N_p)]^{1/2}$.

The anionic dicopper(II) complex of **1** is a novel metallamacrocycle of the dicoppertetraaza[3.3]4,4′-diphenylethynophane-type, where the two 4,4′-diphenylethyne spacers of the bis(bidentate) dpeba bridging ligands are connected by two N−Cu−N linkages (Figure 1a). The two centrosymmetrically related Cu(1) and Cu(1)^{I} atoms adopt a essentially square planar geometry. The CuN_2O_2 coordination environment is defined by two amidate-nitrogen and two carboxylate-oxygen atoms from the oxamato donor groups. The value of the tetrahedral twist angle (τ) between the Cu(1)N(1)O(1) and Cu(1)N(2)O(4) mean planes is 9.4(1)°.

Within the dinuclear metallacyclic core of **1**, $Cu^{II}_2(p\text{-}N_2C_{14}H_8)_2$, each of the two 4,4′-diphenylethyne spacers is almost planar, thus reflecting potential extended π-conjugation for the dpeba bridging ligands. The torsion angle (ψ) between the terminal benzene rings around the central carbon−carbon triple bond is 7.8(1)°. This situation contrasts with that found for the related dicopper(II) metallacyclophane with 4,4′-diphenylene spacers, whereby the phenylene rings are significantly tilted around the carbon−carbon single bond because of the repulsive interactions between the ortho−ortho′ benzene hydrogen atoms (ψ = 19.7°).[13b] The two 4,4′-diphenylethyne spacers of **1** show an offset (non-eclipsed) disposition because of the parallel-displaced π-stacked arrangement of the two pairs of facing benzene rings (Figure 1b). Hence, the molecule has an approximate C_{2h} symmetry, whereby the copper mean basal planes are not exactly oriented perpendicular to the benzene planes [dihedral angles (ϕ) of 56.4(1) and 58.4(1)°] (Figure 1c). Deviations from the ideal D_{2h} molecular symmetry (ψ = 0° and ϕ = 90°) may originate

dx.doi.org/10.1021/ic400754m | Inorg. Chem. 2013, 52, 7645−7657

Table 2. Selected Bond Distances (Å) and Angles (deg) for 1[a]

bond	Å	bond	Å
Cu(1)−N(1)	1.993(3)	Cu(1)−N(2)	1.994(3)
Cu(1)−O(1)	1.948(3)	Cu(1)−O(4)	1.973(3)
angle	deg	angle	deg
N(1)−Cu(1)−N(2)	108.43(13)	N(1)−Cu(1)−O(1)	83.92(12)
N(1)−Cu(1)−O(4)	167.80(12)	N(2)−Cu(1)−O(1)	165.63(12)
N(2)−Cu(1)−O(4)	83.24(12)	O(1)−Cu(1)−O(4)	85.01(11)

[a]The estimated standard deviations are given in parentheses.

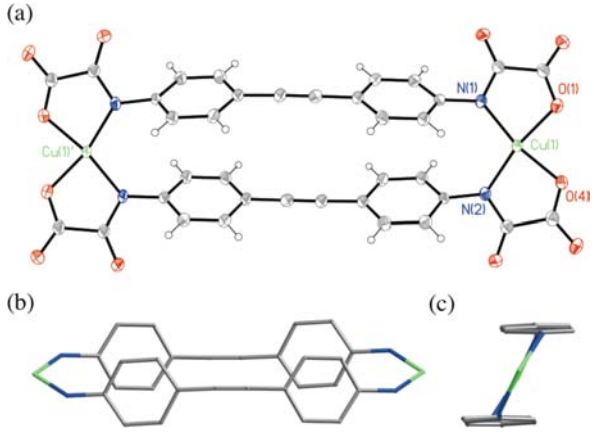

Figure 1. (a) ORTEP drawing of the centrosymmetric anionic dicopper unit of **1** with the atom-numbering scheme of the metal environment [symmetry code: (I) = 2 − *x*, 1 − *y*, 2 − *z*]. The thermal ellipsoids are drawn at the 50% probability level. (b) Front and (c) top projection views of the metallacyclic core of **1**.

from the favorable $\pi-\pi$ interactions in the parallel-displaced configuration of the 4,4′-diphenylethyne spacers.

Spectroscopic Properties. The electronic absorption spectra of **1** and **2** in acetonitrile solution show a common pattern consisting of one broad and intense band in the near UV region, together with two distinct shoulders that extend into the visible zone, whose intensity vary almost proportionally with the number of phenylethyne groups in the OPE spacer (Figure 2a and b). The main peak centered at 308 (**1**)/316 nm (**2**) and the two shoulders located around 340 (**1**)/365 nm (**2**) and 360 (**1**)/385 nm (**2**) are typical of intraligand (IL) $\pi-\pi^*$ transitions within the OPE spacers (Table 3).[15c] In fact, they are also present in somewhat perturbed yet identifiable form with almost half intensity in the electronic absorption spectra of

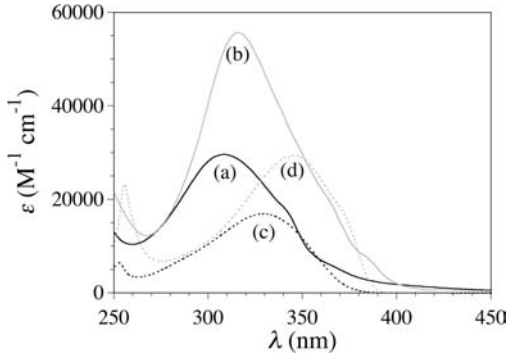

Figure 2. UV−vis spectra of **1** (a) and **2** (b) in acetonitrile solution compared with those of Et_2H_2dpeba (c) and Et_2H_2tpeba (d) in dimethylsulfoxide.

Table 3. Selected UV−Vis Spectroscopic Data for 1 and 2 and the Corresponding Proligands

cmpd	$\lambda_1{}^c$ (nm)	$\lambda_2{}^c$ (nm)	$\lambda_3{}^c$ (nm)
1[a]	308 (29710) [32468]	340 (18850) [29412]	360 (7065) [27778]
2[a]	316 (55815) [31646]	365 (22375) [27397]	385 (7770) [25974]
Et_2H_2dpeba[b]	330 (17015) [30303]	355 (9180) [28169]	
Et_2H_2tpeba[b]	345 (29480) [28986]	370 (18140) [27027]	

[a]In acetonitrile solution at room temperature. [b]In dimethylsulfoxide solution at room temperature. [c]The values of the molar extinction coefficient (ε in M^{-1} cm^{-1} units) and the transition energy ($\nu_i = 1/\lambda_i$ in cm^{-1} units) are given in parentheses and brackets, respectively.

the Et_2H_2dpeba and Et_2H_2tpeba proligands in dimethylsulfoxide (Figure 2c and d). In fact, they show a broad and intense band centered at 330 (Et_2H_2dpeba)/345 nm (Et_2H_2tpeba) with a distinct shoulder located around 355 (Et_2H_2dpeba)/370 nm (Et_2H_2tpeba) (Table 3). More importantly, the relatively large bathochromic shift in the position of these IL bands for both the complexes ($\Delta\nu_1$ = 822 cm^{-1}, $\Delta\nu_2$ = 2015 cm^{-1}, and $\Delta\nu_3$ = 1804 cm^{-1}; Table 3) and the proligands ($\Delta\nu_1$ = 1317 cm^{-1} and $\Delta\nu_2$ = 1142 cm^{-1}; Table 3) is as expected for the increase in the effective π-conjugation length upon increasing the number of phenylethyne units (n) from 1 to 2 in the OPE spacer.

The X-band EPR spectra of frozen-matrix acetonitrile solutions of **1** and **2** at 4.0 K consist of a rhombic signal with a complex multiline splitting pattern which is typical of antiferromagnetically coupled dinuclear copper(II) complexes (Figure 3). In fact, a seven-line splitting of the g_z signal due to the hyperfine coupling with the nuclear spins of the two Cu^{II} ions ($2nI_{Cu} + 1 = 7$ with $n = 2$ and $I_{Cu} = 3/2$) occurs when the magnetic coupling parameter is much larger than the electron−nucleus hyperfine coupling constant ($|J| \gg A_{Cu}$). In contrast, a magnetically uncoupled dinuclear copper(II) complex ($|J| \ll A_{Cu}$) would give an EPR spectrum formally identical to that of a mononuclear one with a simple four-line splitting resulting from the hyperfine coupling with the nuclear spin of the magnetically isolated Cu^{II} ions ($2I_{Cu} + 1 = 4$ with $I_{Cu} = 3/2$).

These EPR spectral features of **1** and **2** were satisfactorily simulated by using the XSOPHE program[16] that diagonalizes the full Hamiltonian matrix within the basis of the three $S = 1$ spin functions ($M_s = 0, \pm 1$) of the $Cu^{II}{}_2$ unit resulting from the antiferromagnetic interaction between the two spin doublets ($S_{Cu} = 1/2$) of each Cu^{II} ion (Figure S2, SI). The calculated values of the Zeeman factors associated with the x, y, and z components of the allowed $M_s = 0 \rightarrow M_s = \pm 1$ transitions for the excited triplet ($S = 1$) spin state of **1**/**2** are g_x = 2.044/2.045, g_y = 2.070/2.065, and g_z = 2.240/2.216, while those of

dx.doi.org/10.1021/ic400754m | Inorg. Chem. 2013, 52, 7645−7657

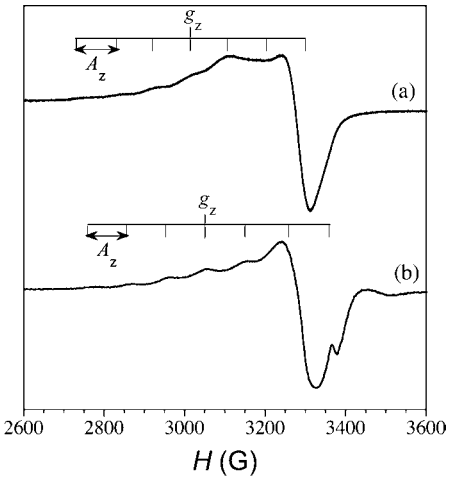

Figure 3. X-band EPR spectra of the frozen-matrix acetonitrile solutions of **1** (a) and **2** (b) at 4.0 K.

the corresponding hyperfine coupling constants are A_x = 20/10 G, A_y = 5/20 G, and A_z = 134/143 G (Table 4). The electron–

Table 4. Selected EPR Spectroscopic Data for 1 and 2[a]

cmpd	g_x[b]	g_y[b]	g_z[b]
1	2.044 (20)	2.070 (5)	2.240 (134)
	[0.0019]	[0.0005]	[0.0138]
2	2.045 (10)	2.065 (20)	2.216 (143)
	[0.0010]	[0.0019]	[0.0148]

[a]In acetonitrile solution at 4.0 K. [b]The values of the Zeeman factors (g_i) and the hyperfine coupling constants (A_i) associated with the x, y, and z components of the allowed $M_s = 0 \rightarrow M_s = \pm 1$ transitions of the excited triplet (S = 1) spin state were calculated by using the XSOPHE program. The calculated A_i values in G and cm^{-1} units are given in parentheses and brackets, respectively.

nucleus hyperfine coupling constant of **1** and **2** can then be estimated from the calculated A_z values resulting from the simulation of the EPR spectra as $A_z = 1/2A_{Cu}$.[17] The calculated anisotropic A_{Cu} values of 268 (**1**) and 286 G (**2**) are similar, as expected for antiferromagnetically coupled dinuclear copper(II) complexes with the same type of ligands, and they give a minimum value for the magnetic coupling parameter of **1** and **2** [$|J| \gg A_{Cu}$ = 0.0276 (**1**) and 0.0296 cm^{-1} (**2**)].

Magnetic Properties. The magnetic properties of **1** and **2** in the form of the χ_M and $\chi_M T$ vs T plots (χ_M being the molar magnetic susceptibility per dinuclear unit and T the absolute temperature) and M vs H plots (M being the molar magnetization per dinuclear unit and H the applied magnetic field) conform with moderate (**1**) to weak (**2**) antiferromagnetically coupled Cu^{II}_2 units, both in the solid state and in solution (Figures 4 and 5). At room temperature, $\chi_M T$ of the polycrystalline samples of **1** and **2** is equal to 0.84 $cm^3\ mol^{-1}$ K, a value which is close to that expected for two magnetically isolated Cu^{II} ions [$\chi_M T = 2 \times (N\beta^2 g_{Cu}{}^2/3k_B) S_{Cu}(S_{Cu} + 1)$ = 0.83 $cm^3\ mol^{-1}$ K with S_{Cu} = 1/2 and g_{Cu} = 2.1, where N is the Avogadro number, β is the Bohr magneton, and k_B is the Boltzmann constant]. Upon cooling, $\chi_M T$ of the polycrystalline sample and frozen-matrix methanol solution of **1** remains constant until ~50 K and then it decreases abruptly to reach values of 0.22 and 0.18 $cm^3\ mol^{-1}$ K respectively, at 2.0 K (Figure 4). By comparison, $\chi_M T$ of the polycrystalline sample and frozen-matrix methanol solution of **2** remains constant

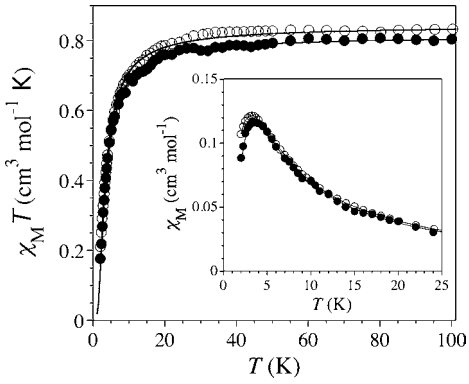

Figure 4. Temperature dependence of $\chi_M T$ of the polycrystalline sample (○) and frozen-matrix methanol solution (●) of **1** under applied magnetic fields of 100 G (T < 25 K) and 1.0 T ($T \geq$ 25 K). The inset shows the temperature dependence of χ_M of the polycrystalline sample (○) and frozen-matrix methanol solution (●) of **1**. The solid lines are the best-fit curves (see text).

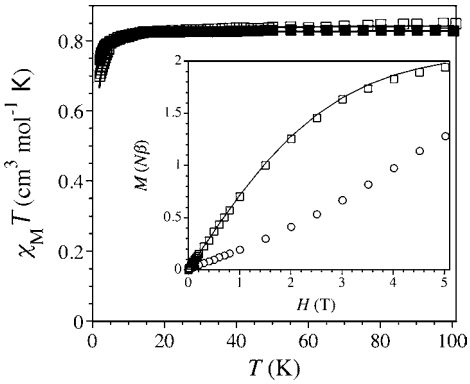

Figure 5. Temperature dependence of $\chi_M T$ of the polycrystalline samples (□) and frozen-matrix methanol solution (■) of **2** under applied magnetic fields of 100 G (T < 25 K) and 1.0 T ($T \geq$ 25 K). The solid lines are the best-fit curves (see text). The inset shows the field dependence of M of the polycrystalline samples of **1** (○) and **2** (□) at 2.0 K. The solid line corresponds to the Brillouin curve for the sum of two doublet spin states (see text).

until ~20 K and then it decreases slightly to reach values of 0.70 and 0.75 $cm^3\ mol^{-1}$ K respectively, at 2.0 K (Figure 5). In addition, the polycrystalline sample and frozen-matrix methanol solution of **1** show a χ_M maximum at 3.3 and 3.5 K respectively (inset of Figure 4), which unambiguously supports the occurrence of a ground singlet (S = 0) spin state resulting from the antiferromagnetic interaction between the two spin doublets (S_{Cu} = 1/2) of each Cu^{II} ion within the Cu^{II}_2 units. Otherwise, the isothermal magnetization curve at 2.0 K of the polycrystalline sample of **1** is well below that of the Brillouin function for two doublet spin states of two magnetically isolated Cu^{II} ions (S_{Cu} = 1/2 with g = 2.1), while it is only slightly below for **2** reflecting thus the different magnitude of the antiferromagnetic coupling in each case (inset of Figure 5).

The analysis of the magnetic susceptibility data of **1** and **2**, both in the solid state and in solution, was carried out through the spin Hamiltonian for a dinuclear copper(II) complex (eq 1 with $S_1 = S_2 = S_{Cu}$ = 1/2), where J is the magnetic coupling parameter and g is the Zeeman factor of the Cu^{II} ions ($g = g_1 = g_2 = g_{Cu}$). The least-squares fits of the experimental data of the polycrystalline samples of **1**/**2** through the well-known Bleaney–Bowers expression (eq 2) gave $-J$ = 3.87(3)/

dx.doi.org/10.1021/ic400754m | Inorg. Chem. 2013, 52, 7645–7657

0.90(1) cm^{-1} and g = 2.124(3)/2.122(1) with $R = 1.5 \times 10^{-5}$/1.0×10^{-5}, while they gave $-J$ = 4.05(3)/0.48(1) cm^{-1} and g = 2.105(3)/2.105(1) with $R = 1.8 \times 10^{-5}/1.5 \times 10^{-5}$ for the frozen-matrix methanol solutions of **1**/**2** (Table 5). The

Table 5. Selected Magnetic Data for 1 and 2[a]

cmpd	J[b] (cm^{-1})	g[c]	R[d] $\times 10^{-5}$
1	−3.87(3)	2.124(3)	1.5
	[−4.05(3)]	[2.105(3)]	[1.8]
2	−0.90(1)	2.122(1)	1.0
	[−0.48(1)]	[2.105(1)]	[1.5]

[a]In the solid state. The magnetic data in methanol solution are given in brackets. [b]Magnetic coupling parameter (see eq 1). The calculated errors are given in parentheses. [c]Zeeman factor of the Cu^{II} ions (see eq 1). The calculated errors are given in parentheses. [d]Agreement factor defined as $R = \sum[(\chi_M T)_{exp} - (\chi_M T)_{calcd}]^2/\sum[(\chi_M T)_{exp}]^2$.

theoretical curves match very well the experimental ones for **1** and **2** (solid lines in Figures 4 and 5) and particularly, they reproduce the observed maximum of χ_M for **1** both in the solid state and in solution (solid lines in the inset of Figure 4). Indeed, the similar magnetic behavior in the solid state and in solution for both **1** and **2** unambiguously demonstrates that the magnetic coupling is intramolecular in origin, the intermolecular interactions in the solid state, if any, being negligible. So, the slight deviations between the $-J$ values in the solid state and in solution for **2** would be most likely due to very small variations of the molecular geometry in each medium.

$$\mathbf{H} = -JS_1 \cdot S_2 + g\beta(S_1 + S_2)H \quad (1)$$

$$\chi_M T = (2N\beta^2 g^2/k_B)/[3 + \exp(-J/k_B T)] \quad (2)$$

The moderate antiferromagnetic coupling for **1** ($-J$ = 3.9−4.1 cm^{-1}) is quite remarkable given the large Cu−Cu separation across the two 4,4′-diphenylethynediamidate bridges ($r \approx$ 15.0 Å). By comparison, the $-J$ values for **1** are only slightly smaller than those reported earlier for related oxamato-based dicopper(II) metallacyclophanes with 4,4′-diphenylene spacers ($-J$ = 8.7−11.5 cm^{-1}) having a rather shorter intermetallic distance (r = 12.2 Å).[13b] Yet the weak but non-negligible antiferromagnetic coupling for **2** ($-J$ = 0.5−0.9 cm^{-1}) is really noticeable given the very long intermetallic distance through the two 1,4-di(4-phenylethynyl)-phenylenediamidate bridges ($r \approx$ 22.0 Å). To our knowledge, **2** is the exchange-coupled dinuclear copper(II) complex with the largest intermetallic distance for which EE effects has been evidenced, showing thus that one nanometer was definitely not the upper limit for the observation of magnetic coupling in dinuclear copper(II) complexes.[2] At this respect, we have recently reported a quite rare *p*-triphenylenediamine-bridged dinuclear copper(II) complex possessing a similarly weak intramolecular antiferromagnetic coupling ($J = -2.0$ cm^{-1}) but with a rather shorter intermetallic distance ($r \approx$ 16.4 Å).[8f]

The moderate to weak, long-range antiferromagnetic coupling in **1** and **2** indicates that strongly delocalized π-type orbital pathways through the para substituted diphenylethyne (**1**) and di(phenylethynyl)phenylene (**2**) spacers are involved, as previously observed for the related oxamato-based dicopper(II) metallacyclophanes with para substituted phenylene spacers which show a strong antiferromagnetic coupling ($-J$ = 81−95 cm^{-1}).[13b] As a matter of fact, the magnetic coupling along this series decreases with the number of phenylethyne repeat units on the organic spacer, $-C_6H_4(C{\equiv}CC_6H_4)_n-$ (n = 0−2). So, the strong antiferromagnetic coupling across the *p*-phenylene spacers (n = 0) previously reported for the parent oxamato-based dicopper(II) paracyclophane ($-J$ = 81−95 cm^{-1})[13b] is no more than 25- and 100-fold those observed for **1** ($-J$ = 3.9−4.1 cm^{-1}) and **2** ($-J$ = 0.5−0.9 cm^{-1}) through the *p*-diphenylethyne (n = 1) and *p*-di(phenylethynyl)-phenylene (n = 2) spacers, respectively. This situation clearly contrasts with that predicted by Coffman and Buettner ($-J$ < 1.0 cm^{-1} at r > 9.0 Å),[2b] showing thus that OPE spacers can act as effective antiferromagnetic wires for the propagation of EE interactions between two Cu^{II} ions separated by intermetallic distances greater than one nanometer.

Energy and Molecular Orbital Calculations: Distance Dependence of Magnetic Coupling. DF calculations were performed in acetonitrile solution on the BS singlet (S = 0) and triplet (S = 1) spin states of the model complexes **1**−**5** with an imposed coplanar conformation of the para substituted benzene rings connected by carbon−carbon triple bonds ($\psi = 0°$) and a perpendicular orientation of the benzene rings with respect to the copper mean basal planes ($\phi = 90°$) (see Computational Details). Selected calculated structural and energy data are listed in Table 6.

Table 6. Selected Calculated Magneto-Structural Data for 1−5[a]

cmpd	r[b] (Å)	ΔE_{ST}[c] (cm^{-1})	δ[d] (cm^{-1})
1	15.266	10.399	927.54
2	21.979	1.095	338.75
3	29.069	0.119	120.98
4	35.931	0.013	40.33
5	42.833	0.002	16.13

[a]DF calculations were performed on the BS singlet (S = 0) and triplet (S = 1) states of the D_{2h}-symmetric model complexes **1**−**5** ($\phi = 90°$ and $\psi = 0°$, see Computational Details). [b]Intermetallic distance. [c]Singlet−triplet energy gap ($\Delta E_{ST} = -J$). [d]Energy gap between the two singly occupied molecular orbitals (SOMOs) for the triplet state.

For all these orthogonal model molecules with an ideal D_{2h} symmetry ($\psi = 0°$ and $\phi = 90°$), the DF energy calculations showed a ground singlet spin state lying below the excited triplet spin state. The calculated value of the singlet−triplet energy gap for the orthogonal model complexes **1** and **2** decreases when increasing the intermetallic distance [$\Delta E_{ST} = -J$ = 10.399 (**1**) and 1.095 cm^{-1} (**2**) for r = 15.095 (**1**) and 21.979 Å (**2**); Table 6], as experimentally observed. The deviations between the calculated and the experimental $-J$ values [$-J$ = 3.9−4.1 (**1**) and 0.5−0.9 cm^{-1} (**2**); Table 5] are likely due to the loss of π-conjugation between the benzene rings by conformational rotation about the carbon−carbon triple bond ($\psi \neq 0°$) and/or the loss of orthogonality between the benzene and the copper mean basal planes ($\phi \neq 90°$), as shown earlier for the related oxamato-based dicopper(II) metallacyclophanes with 4,4′-biphenylene spacers.[13b] In fact, DF energy calculations on the actual structure of **1** possessing an overall parallel-displaced π-stacked conformation of the two not exactly planar 4,4′-diphenylethyne spacers [ψ = 7.8(1)°; ϕ = 56.4(1) and 58.4(1)°] gave a smaller singlet−triplet energy gap ($\Delta E_{ST} = -J$ = 6.1 cm^{-1}) which is closer to the experimental one in the solid state ($-J$ = 3.9 cm^{-1}).[13e] Nevertheless, two nanometers appears to be the upper limit for the observation of magnetic coupling ($-J$ < 1.0 cm^{-1}) in the longer homologues

dx.doi.org/10.1021/ic400754m | Inorg. Chem. 2013, 52, 7645−7657

3−**5** including several C≡C bonds in the OPE spacers, $-C_6H_4(C{\equiv}CC_6H_4)_n-$ (n = 3−5). So, for instance, the DF energy calculations indicate an almost negligible singlet−triplet energy gap between the two Cu^{II} ions separated by up to 28.868 Å through the 4,4′-di(4-phenylethynyl)diphenylethyne spacers in **3** ($\Delta E_{ST} = -J = 0.119$ cm^{-1}).

The results of the DF calculations on the D_{2h}-symmetric model complexes **1**−**5** with extended π-conjugated OPE spacers, $-C_6H_4(C{\equiv}CC_6H_4)_n-$ (n = 1−5), are shown in Figure 6 in terms of both structural and magnetic data.

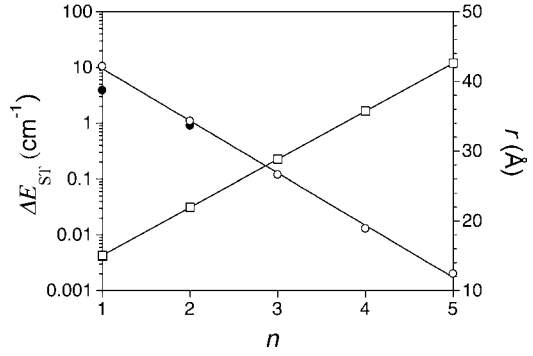

Figure 6. Dependence of the calculated singlet−triplet energy gap (on a semilog scale) (○) and the intermetallic distance (□) for **1**−**5** (data from Table 6) with the number of repeating units in the OPE spacers, $-C_6H_4(C{\equiv}CC_6H_4)_n-$ (n = 1−5). The experimental values of $-J$ (●) and r (■) for the polycrystalline samples of **1** and **2** are also shown for comparison (data from Table 5). The solid lines correspond to the best-fit curves (see text).

Together with a linear increase in the estimated intermetallic distance (r), the calculated singlet−triplet energy gap ($-J$) decreases in an exponential manner with the number of phenylene repeat units (n = 1−5) connected by C≡C bonds along this series (solid lines in Figure 6). The fit of the calculated magneto-structural data for **1**−**5** provides a decay law of the exchange interaction with the intermetallic distance as $-J = 1.08 \times 10^3 \exp(-0.31r)$ (Figure 7). The calculated value of 0.31 $Å^{-1}$ for the exponential factor (γ) is lower than that found in the related series of oxamato-based dicopper(II) metallacyclophanes with *p*-substituted oligophenylene (OP) spacers (γ = 0.35 $Å^{-1}$) (solid lines in Figure 7).[13b] This indicates a higher efficiency on long-range magnetic coupling for the OPE spacers compared to the OP ones, suggesting thus that the inclusion of additional C≡C bonds between the benzene rings occurs without any loss of π-conjugated aromatic character. In fact, the calculated γ value for **1**−**5** is identical to that found in the fully π-conjugated β,β'-substituted oligoacene (OA) spacers (γ = 0.31 $Å^{-1}$), being significantly lower than that found in α,α'-substituted ones (γ = 0.45 $Å^{-1}$) (solid lines in Figure 7).[13c] However, no unique wire-like magnetic behavior was observed for **1**−**5**, as reported earlier for the longer members of the series of oxamato-based dicopper(II) metallacyclophanes with fully π-conjugated OA spacers (Figure 7).[13c]

In contrast, the earlier relationship obtained by Coffman and Buettner[2b] and the subsequent one reported by some of us,[13b] which were based on experimental magneto-structural data on simple dicopper(II) complexes, predict a dramatically faster decay of the magnetic coupling with the intermetallic distance (γ = 1.5−1.8 $Å^{-1}$) (dashed and dotted lines in Figure 7). A remarkable exception is the series of oligo-*p*-phenylenediamine-bridged dicopper(II) complexes recently reported by some of us showing a much slower exponential decay rate of the magnetic coupling which is, however, somewhat higher than that predicted by the DF calculations (γ = 0.37 vs 0.18 $Å^{-1}$).[8f] Fabre et al. also reported the occurrence of strong exchange coupling interactions in Ru^{III}_2 complexes with oligophenyl-, oligophenylethene-, and oligophenylethynedicyanamido bridging ligands (γ = 0.10 $Å^{-1}$),[7k] as predicted theoretically by Ruiz et al. for related oligoacenedicyanamido-bridged M^{III}_2 complexes (M = Cr, Mn, and Fe).[8b] Once again, this reflects the relative efficiency of π- vs σ-type exchange pathways, as expected because of the larger spin delocalization and spin polarization contributions to the ground state electronic structure in the former case.

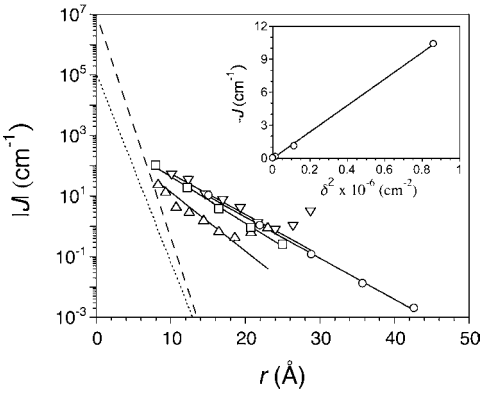

Figure 7. Decay law of the calculated magnetic coupling (J) with the intermetallic distance (r) for **1**−**5** (○) (data from Table 6) compared with those of related oxamato-based dicopper(II) metallacyclophanes with *p*-substituted oligophenylene (□) and α,α'- (Δ) or β,β'-substituted (∇) oligoacene spacers. The inset shows the linear dependence of the calculated values of $-J$ (○) with the square of the energy gap between the two SOMOs (δ) for **1**−**5** (data from Table 6). The solid lines correspond to the best-fit curves, while the dashed and dotted lines are the well-known Coffman−Buettner and related relationships based on experimental magneto-structural data on simple dinuclear copper(II) complexes (see text).

Molecular orbital (MO) calculations on the D_{2h}-symmetric model complexes **1**−**5** provide evidence that the exchange interaction between the two unpaired electrons occupying the σ-type d_{xy} orbitals of the square planar Cu^{II} ions ('magnetic orbitals') and pointing toward the equatorial Cu−N and Cu−O bonds, is mainly transmitted through the π-bond system of the OPE spacers, $-C_6H_4(C{\equiv}CC_6H_4)_n-$ (n = 1−5) (see Scheme 1d). This is nicely illustrated by the pair of singly occupied molecular orbitals (SOMOs) for the triplet spin state of **1** and **2**, which show a high metal−ligand covalency and strongly ligand delocalized character (Figure 8). These two pairs of SOMOs, noted b_{1g} and b_{2u}* (**1**) or alternatively b_{2u} and b_{1g}* (**2**), are composed by the symmetric and antisymmetric combinations of the d_{xy}(Cu) orbitals mixed with the corresponding combinations of appropriate symmetry of the two π-type orbitals of the diphenylethyne (**1**) and di(phenylethynyl)phenylene (**2**) spacers, which are in turn made up of p_z(C) orbitals of the sp^2- and sp-type carbon atoms from the benzene rings and from the ethyne groups, respectively. As expected, the energy gap (δ) between the two SOMOs for the triplet spin state of **1**−**5** decreases continuously along this series (Table 6), in such a way that the calculated $-J$ values vary fairly well with the square of δ as $-J = 12.0 \times 10^{-6}$ δ^2 (inset of Figure 7), according to the simplest orbital models of the electron exchange interaction.[2a] This situation reflects

dx.doi.org/10.1021/ic400754m | Inorg. Chem. 2013, 52, 7645−7657

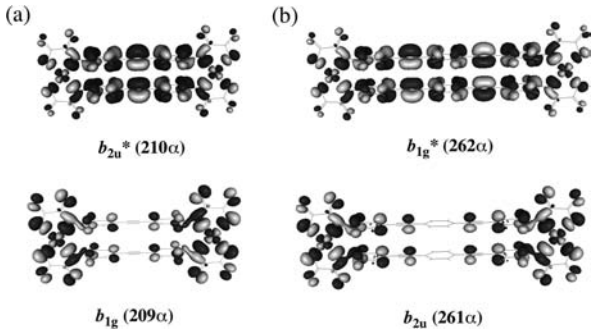

Figure 8. Perspective views of the calculated magnetically active SOMOs for the triplet spin state of **1** (a) and **2** (b). The isodensity surface corresponds to a value of 0.04 e bohr^{-3}.

the parallel decrease of the d_{xy}(Cu)/π(L) metal−ligand orbital mixing for **1**−**5** and, consequently, the smaller delocalization of the unpaired electrons of the Cu^{II} ions onto the π-conjugated electron system of the OPE spacers with the increasing number of phenylethyne units (n) from **1** to **5** along this series.

Spin Density Analysis: Spin Delocalization vs Spin Polarization Mechanism of Magnetic Coupling. Spin densities obtained by natural bond orbital (NBO) analysis on the BS singlet state of **1** and **2** reflect the relative importance of spin delocalization and spin polarization effects for the propagation of the exchange interaction between the unpaired electrons of the two metal centers through the π-type orbital pathways of the *p*-diphenylethyne- (**1**) and *p*-di(phenylethynyl)phenylenediamidate (**2**) bridges (Figure 9).

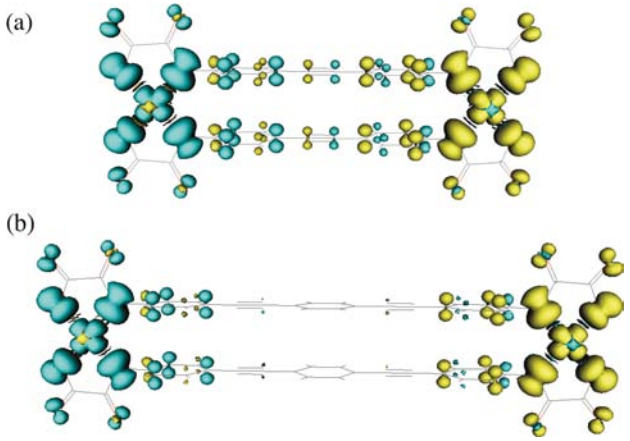

Figure 9. Perspective views of the calculated spin density distribution for the BS singlet spin state of **1** (a) and **2** (b). Yellow and blue contours represent positive and negative spin densities, respectively. The isodensity surface corresponds to a value of 0.001 e bohr^{-3}.

The values of the spin density at the amidate-nitrogen atoms are important [±0.101 (**1**) and ±0.100 e (**2**)] and, moreover, they have the same sign as in the copper atoms to which they are coordinated [±0.564 (**1**) and ±0.565 e (**2**)] (Scheme 3). This fact indicates that the spin delocalization from the metal toward the amidato donor groups dominates over the spin polarization because of the strong covalency of the Cu−N bonds. In contrast, the sign alternation of the spin density at the carbon atoms of the *p*-diphenylethyne- (**1**) and *p*-di(phenylethynyl)phenylene (**2**) spacers agrees with a spin polarization by the amidate-nitrogen atoms, as reported earlier for the related dicopper(II) metallacyclophane with *p*-phenyl-

Scheme 3. Projection View of the Spin Density Distribution on the Oligo(*p*-phenylene-ethynylene)diamidate Bridges for the BS Singlet Spin State of 1 (a) and 2 (b) with the Calculated Atomic Spin Density Values (in e units)[a]

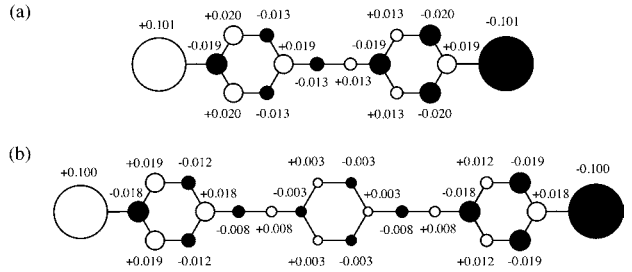

[a]Empty and full circles represent positive and negative spin densities, respectively, with scaled surface areas.

enediamidate bridges.[13b] So, the values of the spin density of opposite sign on the adjacent sp^2-type carbon atoms of the two terminal benzene rings [from ±0.013 to ±0.020 e (**1**) and from ±0.012 to ±0.019 e (**2**)] are as important as those at the sp-type carbon atoms from the ethyne groups to which they are directly attached [±0.013 (**1**) and ±0.008 e (**2**)] (Scheme 3). This situation evidence the partial preservation of the π-conjugation with the incorporation of additional C≡C bonds connecting the phenylene groups into the OPE spacers for **1** and **2**. Indeed, the values of the spin density at the sp^2-type carbon atoms of the central benzene ring in **2** are smaller but non-negligible [±0.003 e] (Scheme 3b), as expected because of the appreciable attenuation of the spin delocalization with the incorporation of an additional phenylene group into the OPE spacers. Hence, a net decrease of the antiferromagnetic exchange interaction results with the successive incorporation of additional phenylethyne units into the OPE spacers, as experimentally observed for **1** and **2** and theoretically predicted for **3** to **5**.

Transition Energy and Molecular Orbital Calculations: Distance Dependence of Intraligand Optical Transitions. TD-DF calculations were performed in acetonitrile solution on the BS singlet (S = 0) and triplet (S = 1) spin states of the D_{2h}-symmetric model complexes **1**−**5** (see Computational Details). Selected calculated structural and transition energy data are listed in Table 7. The MO composition and energy data of the transitions for the triplet spin state of **1**−**4** are shown in Figures S3−S6 (SI), while those of **5** are depicted in Figure 10.

The most remarkable feature of the calculated electronic spectra for the BS singlet and triplet states of the orthogonal model complexes **1**−**5** is the presence of an intense UV band of IL nature. This IL UV band has two main contributions corresponding to the π−π* transitions from the highest occupied molecular orbitals (HOMOs), a_g and b_{2u} (**1**, **3**, and **5**) or alternatively b_{3u} and b_{1g} (**2** and **4**), to the lowest unoccupied molecular orbitals (LUMOs), b_{3u}* and b_{1g}* (**1**, **3**, and **5**) or alternatively a_g* and b_{2u}* (**2** and **4**). The calculated wavenumber (λ_{max}) values increase asymptotically when increasing the correlation length along this series for both the BS singlet and triplet spin states (Figure S7, SI), as experimentally observed [λ_{max} = 308 (**1**) and 316 nm (**2**); Table 3]. A parallel decrease of the calculated values of the HOMO−LUMO energy gap (Δ) corresponding to the two individual π−π* transitions, $a_g \rightarrow b_{3u}$* and $b_{2u} \rightarrow b_{1g}$* (**1**, **3**, and **5**) or alternatively $b_{3u} \rightarrow a_g$* and $b_{1g} \rightarrow b_{2u}$* (**2** and **4**), occurs for the triplet spin state of **1**−**5**. The fit of the calculated

dx.doi.org/10.1021/ic400754m | Inorg. Chem. 2013, 52, 7645−7657

Table 7. Selected Calculated Spectro-Structural Data for 1−5[a]

cmpd	r^b (Å)	$\lambda_{max}{}^c$ (nm) $S = 0$	$\lambda_{max}{}^c$ (nm) $S = 1$
1	15.266	293 (1.24) [34130]	289 (1.08) [34602]
2	21.979	340 (2.60) [29412]	337 (1.94) [29674]
3	29.069	368 (3.14) [27174]	365 (1.73) [27397]
4	35.931	385 (3.69) [25974]	380 (2.88) [26316]
5	42.833	399 (2.38) [25063]	394 (1.65) [25381]

[a]TD-DF calculations were performed on the BS singlet ($S = 0$) and triplet ($S = 1$) states of the D_{2h}-symmetric model complexes **1**−**5** (ϕ = 90° and ψ = 0°, see Computational Details). [b]Intermetallic distance. [c]Intraligand transition wavenumber. The values of the oscillator strength (f) and the transition energy ($\nu_{max} = 1/\lambda_{max}$ in cm^{-1} units) are given in parentheses and brackets, respectively.

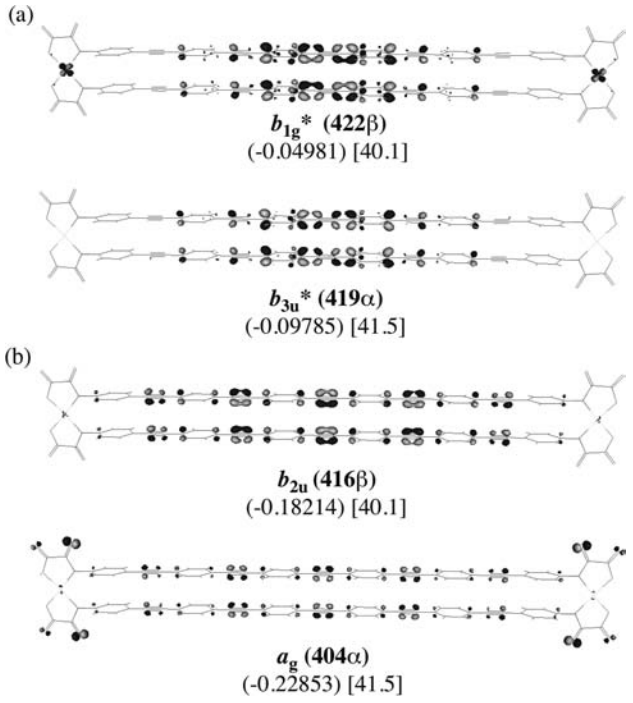

Figure 10. Perspective views of the two calculated pairs of optically active LUMOs (a) and HOMOs (b) involved in the intraligand $\pi-\pi^*$ transitions for the triplet spin state of **5**. The orbital energies (in au) and the transition contribution percentages are given in parentheses and brackets, respectively. The isodensity surface corresponds to a value of 0.04 e $bohr^{-3}$.

spectro-structural data for the BS singlet and triplet spin states of **1**−**5** provides a linear increment law of the IL $\pi-\pi^*$ transition energy with the reciprocal intermetallic distance as $\nu_{max} = 1.99 \times 10^4 + 2.15 \times 10^5\ (1/r)$ ($S = 0$) or $\nu = 2.01 \times 10^4 + 2.18 \times 10^5\ (1/r)$ ($S = 1$) (Figure 11), in such a way that the calculated ν_{max} values vary almost linearly with Δ as $\nu_{max} = 5.7 + 0.90 \times 10^3\Delta$ and $\nu_{max} = -9.7 + 1.52 \times 10^3\Delta$ (inset of Figure 11).

In terms of the ligand field theory, this situation can be described through the π-bonding interaction between the

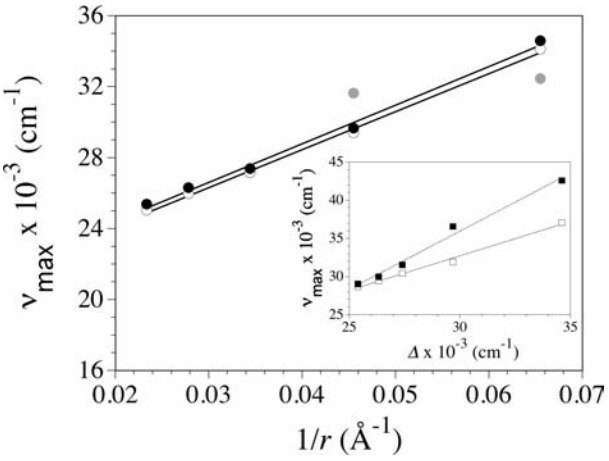

Figure 11. Increment law of the calculated intraligand transition energy (ν_{max}) with the reciprocal intermetallic distance ($1/r$) for the BS singlet (○) and triplet (●) spin states of **1**−**5** (data from Table 7). The experimental values of the intraligand transition energy (●) for **1** and **2** in acetonitrile solution are also shown for comparison (data from Table 3). The inset shows the linear dependence of the calculated ν_{max} values (■) with the HOMO−LUMO energy gap (Δ) of the two optically active a_g/b_{3u}* (□) and b_{2u}/b_{1g}* (■) pairs for the triplet spin state of **1**−**5** (data from Figure 10 and Figures S3−S6, SI). The solid lines are the best-fit curves (see text).

fragment molecular orbitals (FMOs) of the OPE spacers (π_a and π_b) and those of the metal centers (d_{xy} and $d_{x^2-y^2}$), as illustrated for **1** in Scheme 4. The pair of LUMOs, noted b_{3u}* and b_{1g}*, are composed by the symmetric and antisymmetric combinations of the antibonding π_b orbitals of the two facing diphenylethyne spacers, which are weakly mixed with the corresponding combinations of appropriate symmetry of the d_{xy} and $d_{x^2-y^2}$ metal orbitals, respectively. The pair of HOMOs, noted a_g and b_{2u}, are in turn made up by the symmetric and antisymmetric combinations of the bonding π_a orbitals of the two facing diphenylethyne spacers, which are also weakly mixed with the corresponding combinations of appropriate symmetry of the d_{xy} and $d_{x^2-y^2}$ metal orbitals, respectively. These two optically active HOMO/LUMO pairs of mainly ligand-based nature evidence a significant delocalization onto the p_z(C) orbitals of the benzene rings and the ethyne groups that is directly responsible for the proposed molecular wire behavior of extended π-conjugated OPEs,[15c] as exemplified by the longer homologue of this series which shows a strong ligand delocalized character (Figure 10).

■ CONCLUSIONS AND PERSPECTIVES

In this contribution, we present a complementary experimental and density functional study on long-range magnetic and electronic coupling through extended π-conjugated aromatic spacers in a new family of dicopper(II) metallacyclophanes consisting of two square planar bis(oxamato)copper(II) *spin-bearing sites* separated by two linear oligo(*p*-phenyleneethynylene) (OPE) *spacers*, $-C_6H_4(C{\equiv}CC_6H_4)_n-$ (n = 1−5). Because of their planar configuration, a strong orbital overlap between the p_z-type orbitals of the para substituted benzene rings across the carbon−carbon triple bonds occurs along the *p*-phenylethyne *repeat units* of the OPE spacers, as evidenced by the linear increase of the intraligand (IL) $\pi-\pi^*$ transition energy with the reciprocal correlation length along this series. Hence, an unusual π-type orbital pathway is available

dx.doi.org/10.1021/ic400754m | *Inorg. Chem.* 2013, 52, 7645−7657

Scheme 4. Simplified MO Diagram of the π-Bonding Interaction between the Symmetric and Antisymmetric Combinations of the Ligand π_a and π_b and the Metal d_{xy} and $d_{x^2-y^2}$ FMOs for 1[a]

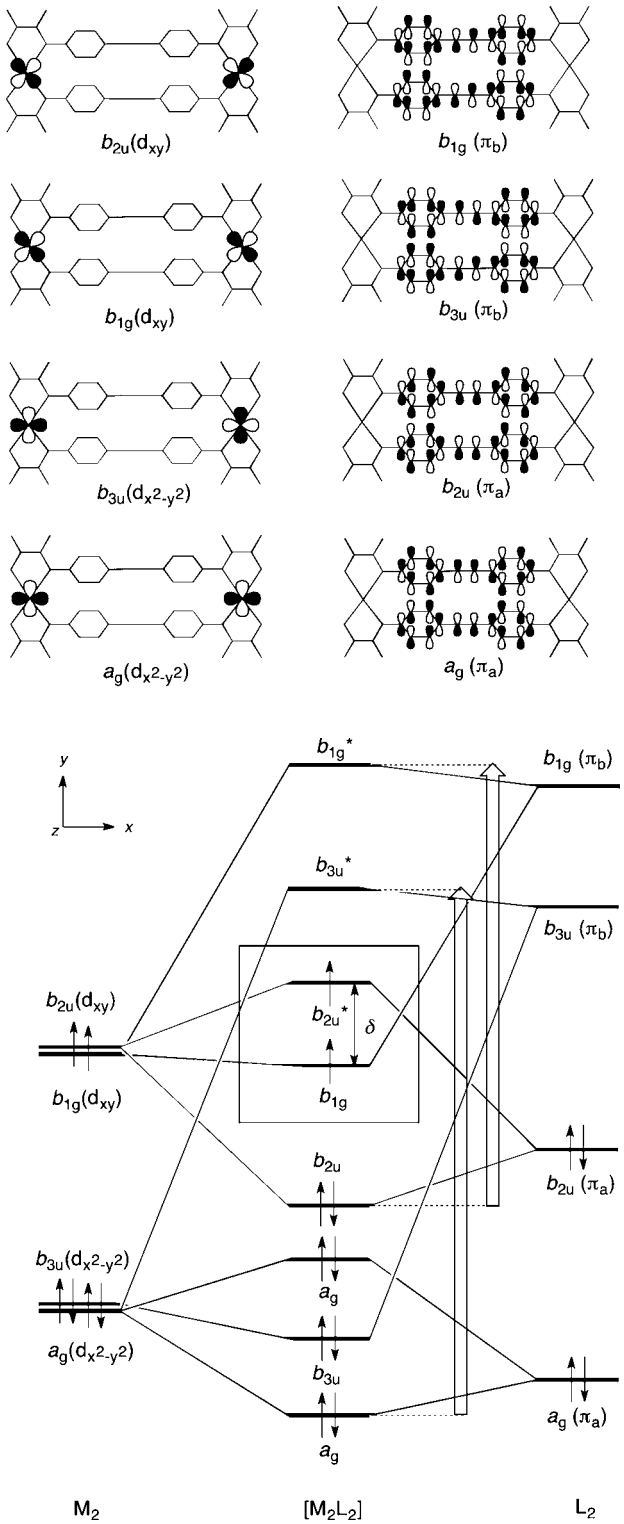

[a]The open arrows correspond to the intraligand $\pi-\pi^*$ transitions between the optically active HOMOs and LUMOs. The boxed structure shows the magnetically active SOMOs.

for the propagation of antiferromagnetic interactions between the unpaired electrons occupying the d_{xy}-type orbitals of the two metal centers through the extended π-conjugated OPE spacers, which are disposed perpendicularly to the metal basal planes as a result of the overall orthogonal molecular geometry. On the other hand, the relatively slow exponential decay of the antiferromagnetic coupling with the intermetallic distance along this series indicates that the EE interactions through linear OPE spacers follows a spin polarization mechanism. This conclusion is further supported by the presence of non-negligible spin densities of alternating sign on the bridge in the calculations on the broken-symmetry (BS) singlet states. On the basis of this combined experimental and computational study, we then propose that linear OPE spacers can act as effective antiferromagnetic wires between two Cu^{II} ions separated by up to 3.0 nm.

We are currently investigating novel series of electro- and photoactive, oxamato-based dicopper(II) metallacyclophanes with extended π-conjugated oligoanthraquinone (OAQ) and oligo-*p*-phenylvinylidene (OPV) spacers as potential candidates for electro- and photoswitchable antiferromagnetic wires, respectively. Indeed, these simple molecules are ideal experimental and theoretical models for the fundamental study on electron- and phototriggered EE processes, which are two central topics in the emerging area of molecular spintronics.[13f,g] Moreover, they appear as very promising candidates to get multifunctional molecule-based magnetic devices facilitating the spin communication ("molecular magnetic wires", MMWs) or exhibiting multistable spin behavior ("molecular magnetic switches", MMSs) for future applications in information processing and storage.

EXPERIMENTAL SECTION

Materials. All chemicals were of reagent-grade quality, and they were purchased from commercial sources and used as received. 4,4′-Diphenylethynediamine and 1,4-di(4-phenylethynyl)-phenylenediamine were prepared as reported in the literature.[15a]

Et_2H_2dpeba. Triethylamine (1.4 mL, 10.0 mmol) and ethyl oxalyl chloride ester (1.2 mL, 10.0 mmol) were added to a solution of 4,4′-diphenylethynediamine (1.0 g, 5.0 mmol) in THF (150 mL) under vigorous stirring. The reaction mixture was heated under reflux for 3 h at 80 °C. The yellow solid was collected by filtration, washed thoroughly with water to remove the precipitate of Et_3NHCl, and then with acetone and diethyl ether, and dried under vacuum (1.6 g, 78% yield). Anal.: Calcd for $C_{22}H_{20}N_2O_6$: C, 64.70; H, 4.94; N, 6.86. Found: C, 64.77; H, 4.97; N, 6.82. ^{1}H NMR (C_2D_6SO): δ 1.32 (t, 6 H, 2 CH_3), 4.31 (q, 4 H, 2 CH_2O), 7.54 (d, 4 H, 2-H, 6-H, 2′-H, and 6′-H), 7.82 (d, 4 H, 3-H, 5-H, 3′-H, and 5′-H), 10.96 (s, 2 H, 2 NH). IR (KBr): 3335 (N−H), 2208 (C≡C), 1729, 1705 cm^{-1} (C═O).

Et_2H_2tpeba. Triethylamine (1.4 mL, 10.0 mmol) and ethyl oxalyl chloride ester (1.2 mL, 10.0 mmol) were added to a solution of 1,4-di(4-phenylethynyl)phenylenediamine (1.5 g, 5.0 mmol) in THF (150 mL) under vigorous stirring. The reaction mixture was heated under reflux for 3 h at 80 °C. The yellow solid was collected by filtration, washed thoroughly first with water to remove the precipitate of Et_3NHCl and then with acetone and diethyl ether, and dried under vacuum (2.0 g, 80% yield). Anal.: Calcd for $C_{30}H_{24}N_2O_6$: C, 70.86; H, 4.76; N, 5.51. Found: C, 70.77; H, 4.82; N, 5.52. ^{1}H NMR (C_2D_6SO): δ 1.33 (t, 6 H, 2 CH_3), 4.35 (q, 4 H, 2 CH_2O), 7.50 (s, 4 H, 2-H, 3-H, 5-H, and 6-H), 7.52 (d, 4 H, 2′-H, 6′-H, 2″-H, and 6″-H), 7.81 (d, 4 H, 3′-H, 5′-H, 3″-H, and 5″-H), 10.99 (s, 2 H, 2 NH). IR (KBr): 3335 (N−H), 2217 (C≡C), 1729, 1698 cm^{-1} (C═O).

(nBu_4N)$_4$[Cu_2(dpeba)$_2$]·4MeOH·2Et_2O (1). A 1.0 M methanolic solution of nBu_4NOH (4.0 mL, 4.0 mmol) was added to a suspension of Et_2H_2dpeba (0.41 g, 1.0 mmol) in 20 mL of methanol under gentle warming. A methanol solution (10 mL) of $Cu(ClO_4)_2·6H_2O$ (0.37 g, 1.0 mmol) was then added dropwise under stirring. The resulting mixture was filtered to remove the small amount of solid particles and

dx.doi.org/10.1021/ic400754m | Inorg. Chem. 2013, 52, 7645−7657

the solvent was removed under vacuum. The dark-green solid was recuperated with THF, collected by filtration, washed thoroughly with THF to remove the precipitate of nBu$_4$NClO$_4$, and air-dried. Recrystallization from a methanol solution gave dark-green prisms of **1** suitable for single-crystal X-ray diffraction upon layering of diethyl ether (0.72 g, 70% yield). Anal.: calcd for $C_{112}H_{196}Cu_2N_8O_{18}$: C, 64.99; H, 9.54; N, 5.41. Found: C, 64.55; H, 9.36; N, 5.32. IR (KBr): 2207 (C≡C), 1685, 1648, 1611 cm^{-1} (C═O).

(nBu$_4$N)$_4$[Cu$_2$(tpeba)$_2$]·12H$_2$O (2). A 1.0 M methanolic solution of nBu$_4$NOH (4.0 mL, 4.0 mmol) was added to a suspension of Et$_2$H$_2$tpeba (0.51 g, 1.0 mmol) in 20 mL of methanol under gentle warming. A methanol solution (10 mL) of Cu(ClO$_4$)$_2$·6H$_2$O (0.37 g, 1.0 mmol) was then added dropwise under stirring. The resulting mixture was filtered to remove the small amount of solid particles, and the solvent was removed under vacuum. A microcrystalline dark-green solid of **2** was recuperated with THF, collected by filtration, washed thoroughly with THF to remove the precipitate of nBu$_4$NClO$_4$, and air-dried (0.70 g, 65% yield). Anal.: calcd for $C_{116}H_{192}Cu_2N_8O_{24}$: C, 63.05; H, 8.76; N, 5.07. Found: C, 63.37; H, 8.63; N, 4.92. IR (KBr): 2208 (C≡C), 1683, 1649, 1619 cm^{-1} (C═O).

Physical Techniques. Elemental analyses (C, H, N) were performed at the Servicio Central de Soporte a la Investigación (SCSIE) at the Universitat de València (Spain). ^{1}H NMR spectra were recorded at room temperature on a Bruker AC 200 (200.1 MHz) spectrometer. Deuterated dimethylsulfoxide was used as solvent and internal standard (δ = 2.50 ppm). FT−IR spectra were recorded on a Nicolet-5700 spectrophotometer as solid KBr pellets. Electronic absorption spectra were recorded on acetonitrile or dimethylsulfoxide solutions at room temperature with an Agilent Technologies-8453 spectrophotometer equipped with a UV−vis Chem Station. X-band (ν = 9.47 GHz) EPR spectra were recorded on frozen-matrix acetonitrile solutions at 4.0 K under nonsaturating conditions with a Bruker ER 200 D spectrometer equipped with a helium cryostat.

Magnetic Measurements. Variable-temperature (2.0−300 K) magnetic susceptibility measurements and variable-field (0−5.0 T) magnetization measurements at 2.0 K were carried out on powdered polycrystalline samples with a SQUID magnetometer. The magnetic susceptibility data at low temperatures (T < 25 K) were measured under a very low applied magnetic field (H = 100 G) in order to avoid saturation effects.

Variable-temperature (2.0−150 K) magnetic susceptibility measurements on frozen-matrix methanol solutions were performed with the same SQUID magnetometer. Two quartz tubes of suprasil quality (8 cm height ×5 mm outer diameter with 0.5 mm wall thickness) were placed together in vertical position, the top tube containing the sample in methanol (8 mm is the height of the solution) and the bottom one being open on both sides. The two tubes fit perfectly in the plastic straw normally used in the SQUID devices. Placing the two tubes one on the top of the other in a vertical manner minimizes their magnetic contribution. In this respect, it is very illustrative that the two empty tubes placed in the plastic straw under an applied magnetic field of 1.0 T gave an almost negligible magnetic signal (less than 5.0 × 10^{-6} cm^3). The experimental data were corrected for the diamagnetic contributions of the constituent atoms and the sample holder and/or the methanol solvent (24000 × 10^{-6} cm^3 mol^{-1}), as well as for the temperature-independent paramagnetism (tip) of the two Cu^{II} ions (120 × 10^{-6} cm^3 mol^{-1}).

Crystal Structure Data Collection and Refinement. Single-crystal X-ray diffraction data of **1** were collected on a Bruker-Nonius X8APEXII CCD area detector diffractometer using graphite-monochromated Mo−K$_\alpha$ radiation. All calculations for data reduction, structure solution, and refinement were done through the SAINT[19] and SADABS[20] programs. The structure of **1** was solved by direct methods and subsequently completed by Fourier recycling using the SHELXTL software package.[21] All non-hydrogen atoms were refined anisotropically. The hydrogen atoms were set in calculated positions and refined as riding atoms. The final geometrical calculations and the graphical manipulations were carried out with PARST97[22] and Crystal Maker[23] programs, respectively.

Crystallographic data (excluding structure factors) of **1** have been deposited with the Cambridge Crystallographic Data Centre as supplementary publication number CCDC-831325. Copies of the data can be obtained free of charge on application to CCDC, 12 Union Road, Cambridge CB21EZ, UK (Fax: (+44) 1223-336-033; e-mail: deposit@ccdc.cam.ac.uk).

Computational Details. The molecular geometries of the model complexes **1**−**5** with D_{2h} molecular symmetry were not optimized, but their bond lengths and interbond angles were taken from the crystal structure of **1** with an imposed coplanar conformation of the phenylene rings in the OPE spacers (ψ = 0°) and a perpendicular orientation of the phenylene rings with respect to the copper mean basal planes (ϕ = 90°).

Density functional (DF) calculations and other ones based on the time-dependent formalism (TD-DF) were carried out on the broken-symmetry (BS) singlet and triplet spin states of the D_{2h}-symmetric model complexes **1**−**5** in acetonitrile solution using the hybrid B3LYP functional[24] combined with the "broken-symmetry" approach,[25] as implemented in the Gaussian 09 program.[26] The triple- and double-ζ quality basis sets proposed by Ahlrichs and co-workers[27] were used for the metal and nonmetal atoms, respectively. The calculated spin density data were obtained from Natural Bond Orbital (NBO) analysis.[28] Solvation effects were introduced using a polarizable continuum model (PCM), where the cavity is created via a series of overlapping spheres,[29] in order to accurately calculate the energy data of the frontier molecular orbitals as well as the transition energy data and transition strength force constants, which were deduced from transition electric dipole moments.

■ ASSOCIATED CONTENT

Ⓢ Supporting Information

Crystal packing view of **1** (Figure S1), simulated X-band EPR spectra of frozen-matrix acetonitrile solutions of **1** and **2** (Figure S2), perspective views of the two pairs of optically active LUMOs and HOMOs for **1**−**4** (Figures S3−S6), and plot of the calculated intraligand transition wavenumber and the HOMO−LUMO energy gaps with the number of repeating units for **1**−**5** (Figure S7). This material is available free of charge via the Internet at http://pubs.acs.org.

■ AUTHOR INFORMATION

Corresponding Author

* E-mail: joan.cano@uv.es (J.C.); francisco.lloret@uv.es (F.L.); donatella.armentano@unical.it (D.A.)

Present Address

$^\perp$University Sidi Mohammed Ben Abdellah, Fes, Morocco.

Notes

The authors declare no competing financial interest.

■ ACKNOWLEDGMENTS

This work was supported by the Ministerio de Ciencia e Innovación (MICINN, Spain) (Projects CTQ2010-15364 and CSD2007-00010), the Generalitat Valenciana (GV, Spain) (Project PROMETEO/2009/108 and ISIC/2012/002), and the Ministero dell'Istruzione, dell'Università e della Ricerca Scientifica (Italy) through the Centro di Eccellenza CEMIF.-CAL (Grant CLAB01TYEF). M.C. and F.R.F.-P. thank the MICINN for doctoral grants. A.B. thanks the GV for a stay grant. We acknowledge J. M. Martínez (Universitat de València) for the assistance and help in EPR data collection.

■ REFERENCES

(1) (a) Kahn, O. *Molecular Magnetism*; VCH Publishers: New York, 1993. (b) Jorner, J., Ratner, M., Eds. *Molecular Electronics*; Blackwell Science: Oxford, 1997.

(2) (a) Hay, J. P.; Thibeault, J. C.; Hoffmann, R. *J. Am. Chem. Soc.* **1975**, *97*, 4884. (b) Coffman, R. E.; Buettner, G. R. *J. Phys. Chem.* **1979**, *83*, 2387. (c) Kahn, O. *Angew. Chem., Int. Ed. Engl.* **1985**, *24*, 834. (d) McCleverty, J. A.; Ward, M. D. *Acc. Chem. Res.* **1998**, *31*, 842. (e) Terencio, T.; Bastardis, R.; Suaud, N.; Maynau, D.; Bonvoisin, J.; Malrieu, J. P.; Calzado, C. J.; Guihéry, N. *Phys. Chem. Chem. Phys.* **2011**, *13*, 12314.

(3) (a) Creutz, C. *Prog. Inorg. Chem.* **1983**, *30*, 1. (b) Crutchley, R. J. *Adv. Inorg. Chem.* **1994**, *41*, 273. (c) Launay, J. P. *Chem. Soc. Rev.* **2001**, *30*, 386. (d) Launay, J. P.; Coudret, C. *Electron Transfer in Chemistry*; Wiley-VCH: Weinheim, Germany, 2001; Vol. *5*, p 3.

(4) (a) Joachim, C.; Gimzewski, J. K.; Aviram, A. *Nature* **2000**, *408*, 541. (b) Tour, J. M. *Acc. Chem. Res.* **2000**, *33*, 791. (c) Caroll, R. R.; Gorman, C. B. *Angew. Chem., Int. Ed.* **2002**, *41*, 4379. (d) Liang, W.; Shores, M. P.; Bockrath, M.; Long, J. R.; Park, H. *Nature* **2002**, *417*, 725. (e) Robertson, N.; McGowan, C. A. *Chem. Soc. Rev.* **2003**, *32*, 96. (f) Dei, A.; Gatteschi, D.; Sangregorio, C.; Sorace, L. *Acc. Chem. Res.* **2004**, *37*, 827. (g) Lafferentz, L.; Ample, F.; Yu, H.; Hecht, S.; Joachim, C.; Grill, L. *Science* **2009**, *323*, 1193.

(5) (a) Dul, M. C.; Pardo, E.; Lezcouëzec, R.; Chamoreau, L. M.; Villain, F.; Journaux, Y.; Ruiz-García, R.; Cano, J.; Julve, M.; Lloret, F.; Pasán, J.; Ruiz-Pérez, C. *J. Am. Chem. Soc.* **2009**, *131*, 14614. (b) Pardo, E.; Ferrando-Soria, J.; Dul, M. C.; Lezcouëzec, R.; Journaux, Y.; Ruiz-García, R.; Cano, J.; Julve, M.; Lloret, F.; Cañadillas-Delgado, L.; Pasán, J.; Ruiz-Pérez, C. *Chem.—Eur. J.* **2010**, *16*, 12838.

(6) (a) Bruce, M. I.; Low, P. J. *Adv. Organomet. Chem.* **2004**, *50*, 179. (b) Aguirre-Etcheverry, P.; O'Hare, D. *Chem. Rev.* **2010**, *110*, 4839.

(7) (a) Felthouse, T. R.; Duesler, E. N.; Hendrickson, D. N. *J. Am. Chem. Soc.* **1978**, *100*, 618. (b) Felthouse, T. R.; Hendrickson, D. N. *Inorg. Chem.* **1978**, *17*, 2636. (c) Chaudhuri, P.; Oder, K.; Wieghardt, K.; Gehring, S.; Haase, W.; Nuber, B.; Weiss, J. *J. Am. Chem. Soc.* **1988**, *110*, 3657. (d) Bürger, K. S.; Chaudhuri, P.; Wieghardt, K.; Nuber, B. *Chem.—Eur. J.* **1995**, *1*, 583. (e) Cargill-Thompson, A. M. W.; Gatteschi, D.; McCleverty, J. A.; Navas, J. A.; Rentschler, E.; Ward, M. D. *Inorg. Chem.* **1996**, *35*, 2701. (f) Ung, V. A.; Cargill-Thompson, A. M. W.; Bardwell, D. A.; Gatteschi, D.; Jeffery, J. C.; McCleverty, J. A.; Totti, F.; Ward, M. D. *Inorg. Chem.* **1997**, *36*, 3447. (g) Cano, J.; De Munno, G.; Sanz, J. L.; Ruiz, R.; Faus, J.; Lloret, F.; Julve, M.; Caneschi, A. *J. Chem. Soc., Dalton Trans.* **1997**, 1915. (h) Ung, V. A.; Couchman, S. M.; Jeffery, J. C.; McCleverty, J. A.; Ward, M. D.; Totti, F.; Gatteschi, D. *Inorg. Chem.* **1999**, *38*, 365. (i) Bayly, S.; McCleverty, J. A.; Ward, M. D.; Gatteschi, D.; Totti, F. *Inorg. Chem.* **2000**, *39*, 1288. (j) Shores, M. P.; Long, J. R. *J. Am. Chem. Soc.* **2002**, *124*, 3512. (k) Fabre, M.; Bonvoisin, J. *J. Am. Chem. Soc.* **2007**, *129*, 1434. (l) Hamon, P.; Justaud, F.; Cador, O.; Hapiot, P.; Rigaut, S.; Toupet, L.; Ouahab, L.; Stueger, H.; Hamon, J.-R.; Lapinte, C. *J. Am. Chem. Soc.* **2008**, *130*, 17372. (m) Rancan, M.; Dolmella, A.; Seraglia, R.; Orlandi, S.; Quici, S.; Sorace, L.; Gatteschi, D.; Armelao, L. *Inorg. Chem.* **2012**, *51*, 5409.

(8) (a) Bencini, A.; Gatteschi, D.; Totti, F.; Nieto-Sanz, D.; McCleverty, J. A.; Ward, M. D. *J. Phys. Chem. A* **1998**, *102*, 10545. (b) Ruiz, E.; Rodríguez-Fortea, A.; Alvarez, S. *Inorg. Chem.* **2003**, *42*, 4881. (c) Nunzi, F.; Ruiz, E.; Cano, J.; Alvarez, S. *J. Phys. Chem. C* **2007**, *111*, 618. (d) Li, W.; Yang, F.; Wang, Z.; Hu, J.; Ma, J. *J. Phys. Chem. A* **2009**, *113*, 3375. (e) Hadt, R. G.; Nemykin, V. N. *Inorg. Chem.* **2009**, *48*, 3982. (f) Ferrando-Soria, J.; Castellano, M.; Yuste, C.; Lloret, F.; Julve, M.; Fabelo, O.; Ruiz-Pérez, C.; Stiriba, S.-E.; Ruiz-García, R.; Cano, J. *Inorg. Chim. Acta* **2010**, *363*, 1666. (g) Yuste, C.; Ferrando-Soria, J.; Cangussu, D.; Fabelo, O.; Ruiz-Pérez, C.; Marino, N.; De Munno, G.; Stiriba, S.-E.; Ruiz-García, R.; Cano, J.; Lloret, F.; Julve, M. *Inorg. Chim. Acta* **2010**, *363*, 1984. (h) Meskaldji, S.; Zaiter, A.; Belkhiri, L.; Boucekkine, A. *Theor. Chem. Acc.* **2012**, *131*, 1151.

(9) (a) Pardo, E.; Ruiz-García, R.; Cano, J.; Ottenwaelder, X.; Lescouëzec, R.; Journaux, Y.; Lloret, F.; Julve, M. *Dalton Trans.* **2008**, 2780. (b) Dul, M. C.; Pardo, E.; Lezcouëzec, R.; Journaux, Y.; Ferrando-Soria, J.; Ruiz-García, R.; Cano, J.; Julve, M.; Lloret, F.; Cangussu, D.; Pereira, C. L. M.; Stumpf, H. O.; Pasán, J.; Ruiz-Pérez, C. *Coord. Chem. Rev.* **2010**, *254*, 2281.

(10) (a) Mederos, A.; Gili, P.; Domínguez, S.; Benítez, A.; Palacios, M. S.; Hernández-Padilla, M.; Martín-Zarza, P.; Rodríguez, M. L.; Ruiz-Pérez, C.; Lahoz, F. J.; Oro, L. A.; Brito, F.; Arrieta, J. M.; Vlassi, M.; Germain, G. *J. Chem. Soc., Dalton Trans.* **1990**, 1477. (b) Domínguez, S.; Mederos, A.; Gili, P.; Rancel, A.; Rivero, A. E.; Brito, F.; Lloret, F.; Solans, X.; Ruiz-Pérez, C.; Rodríguez, M. L.; Brito, I. *Inorg. Chim. Acta* **1997**, *255*, 367.

(11) (a) Bear, C. A.; Waters, J. M.; Waters, T. N. *J. Chem. Soc. A* **1970**, *17*, 2494. (b) Jeter, D. Y.; Hatfield, W. E. *Inorg. Chim. Acta* **1972**, *6*, 440. (c) Hernández-Molina, R.; Mederos, A.; Gili, P.; Domínguez, S.; Lloret, F.; Cano, J.; Julve, M.; Ruiz-Pérez, C.; Solans, X. *J. Chem. Soc., Dalton Trans.* **1997**, 4327. (d) Paital, A. R.; Mitra, T.; Ray, D.; Wong, W. T.; Ribas-Ariño, J.; Novoa, J. J.; Ribas, J.; Aromí, G. *Chem. Commun.* **2005**, 5172. (e) Paital, A. R.; Wu, A. Q.; Guo, G. G.; Aromí, G.; Ribas-Ariño, J.; Ray, D. *Inorg. Chem.* **2007**, *46*, 2947. (f) Vázquez, M.; Taglietti, A.; Gatteschi, D.; Sorace, L.; Sangregorio, C.; González, A. M.; Maneiro, M.; Pedrido, R. M.; Bermejo, M. R. *Chem. Commun.* **2003**, 1840.

(12) (a) Inoue, M. B.; Velázquez, E. F.; Medrano, F.; Ochoa, K. L.; Gálvez, J. C.; Inoue, M.; Fernando, Q. *Inorg. Chem.* **1998**, *37*, 4070. (b) Inoue, M. B.; Muñoz, I. C.; Machi, L.; Inoue, M.; Fernando, Q. *Inorg. Chim. Acta* **2000**, *311*, 50. (c) Inoue, M. B.; Inoue, M.; Sugich-Miranda, R.; Machi, L.; Velázquez, E. F.; Fernando, Q. *Inorg. Chim. Acta* **2001**, *317*, 181. (d) Mosina, L. V.; Raitsimring, A. V.; Inoue, M. B.; Fernando, Q.; Inoue, M. *Appl. Magn. Reson.* **2001**, *20*, 249.

(13) (a) Fernández, I.; Ruiz, R.; Faus, J.; Julve, M.; Lloret, F.; Cano, J.; Ottenwaelder, X.; Journaux, Y.; Muñoz, M. C. *Angew. Chem., Int. Ed.* **2001**, *40*, 3039. (b) Pardo, E.; Faus, J.; Julve, M.; Lloret, F.; Muñoz, M. C.; Cano, J.; Ottenwaelder, X.; Journaux, Y.; Carrasco, R.; Blay, G.; Fernández, I.; Ruiz-García, R. *J. Am. Chem. Soc.* **2003**, *125*, 10770. (c) Pardo, E.; Carrasco, R.; Ruiz-García, R.; Julve, M.; Lloret, F.; Muñoz, M. C.; Journaux, Y.; Ruiz, E.; Cano, J. *J. Am. Chem. Soc.* **2008**, *130*, 576. (d) Pardo, E.; Ferrando-Soria, J.; Dul, M. C.; Lezcouëzec, R.; Journaux, Y.; Ruiz-García, R.; Cano, J.; Julve, M.; Lloret, F.; Cañadillas-Delgado, L.; Pasán, J.; Ruiz-Pérez, C. *Chem.—Eur. J.* **2010**, *16*, 12838. (e) Castellano, M.; Fortéa-Pérez, F. R.; Stiriba, S.-E.; Julve, M.; Lloret, F.; Armentano, D.; De Munno, G.; Ruiz-García, R.; Cano, J. *Inorg. Chem.* **2011**, *50*, 11279. (f) Castellano, M.; Ferrando-Soria, J.; Pardo, E.; Julve, M.; Lloret, F.; Mathonière, C.; Pasán, J.; Ruiz-Pérez, C.; Cañadillas-Delgado, L.; Ruiz-García, R.; Cano, J. *Chem. Commun.* **2011**, *47*, 11035. (g) Ferrando-Soria, J.; Castellano, M.; Ruiz-García, R.; Cano, J.; Julve, M.; Lloret, F.; Pasán, J.; Ruiz-Pérez, C.; Cañadillas-Delgado, L.; Li, Y.; Journaux, Y.; Pardo, E. *Chem. Commun.* **2012**, *48*, 8401.

(14) (a) Schwab, P. F. H.; Levin, M. D.; Michl, J. *Chem. Rev.* **1999**, *99*, 1863. (b) Szafert, S.; Gladysz, J. A. *Chem. Rev.* **2003**, *103*, 4175. (c) Schwab, P. F. H.; Smith, J. R.; Michl, J. *Chem. Rev.* **2005**, *105*, 1197. (d) Ren, T. *Chem. Rev.* **2008**, *108*, 4185.

(15) (a) Deeming, A. J.; Hogarth, G.; Lee, M. V.; Saha, M.; Redmond, S. P.; Phetmung, H. T.; Orpen, A. G. *Inorg. Chim. Acta* **2000**, *309*, 109. (b) McLean, D. G.; Rogers, J. E.; Cooper, T. M. *Proc. SPIE-Int. Soc. Opt. Eng.* **2002**, *11*, 4462. (c) Magyar, R. J.; Tretiak, S.; Gao, Y.; Wang, H.-L.; Shreve, A. P. *Chem. Phys. Lett.* **2005**, *401*, 149. (d) Kaliginedi, C.; Moreno-García, P.; Valkenier, H.; Hong, W.; García-Suárez, V. M.; Buiter, P.; Otten, J. L. H.; Hummelen, J. C.; Lambert, C. J.; Wandlowski, T. *J. Am. Chem. Soc.* **2012**, *134*, 5262 and refs therein..

(16) Hanson, G. R.; Gates, K. E.; Noble, C. J.; Griffin, M.; Mitchell, A.; Benson, S. *J. Inorg. Biochem.* **2004**, *98*, 903 (*XSOPHE*).

(17) Bencini, A.; Gatteschi, D. *EPR of Exchange Coupled Systems*; Springer-Verlag: Berlin, 1990.

(18) Cano, J. *VPMAG Package*; University of Valencia: Valencia, Spain, 2003.

(19) *SAINT*, version 6.45; Bruker Analytical X-ray Systems: Madison, WI, 2003.

(20) Sheldrick, G. M. *SADABS Program for Absorption Correction*, version 2.10; Analytical X-ray Systems: Madison, WI, 2003.

(21) *SHELXTL*; Bruker Analytical X-ray Instruments: Madison, WI, 1998.

(22) Nardelli, M. *J. Appl. Crystallogr.* **1995**, *28*, 659.
(23) Palmer, D. *Crystal Maker*; Cambridge University Technical Services: Cambridge, 1996.
(24) Becke, A. D. *J. Chem. Phys.* **1993**, *98*, 5648.
(25) (a) Ruiz, E.; Cano, J.; Alvarez, S.; Alemany, P. *J. Comput. Chem.* **1999**, *20*, 1391. (b) Ruiz, E.; Rodriguez-Fortea, A.; Cano, J.; Alvarez, S.; Alemany, P. *J. Comput. Chem.* **2003**, *24*, 982.
(26) Frisch, M. J.; Trucks, G. W.; Schlegel, H. B.; Scuseria, G. E.; Robb, M. A.; Cheeseman, J. R.; Scalmani, G.; Barone, V.; Mennucci, B.; Petersson, G. A.; Nakatsuji, H.; Caricato, M.; Li, X.; Hratchian, H. P.; Izmaylov, A. F.; Bloino, J.; Zheng, G.; Sonnenberg, J. L.; Hada, M.; Ehara, M.; Toyota, K.; Fukuda, R.; Hasegawa, J.; Ishida, M.; Nakajima, T.; Honda, Y.; Kitao, O.; Nakai, H.; Vreven, T.; Montgomery, J. A., Jr.; Peralta, J. E.; Ogliaro, F.; Bearpark, M.; Heyd, J. J.; Brothers, E.; Kudin, K. N.; Staroverov, V. N.; Kobayashi, R.; Normand, J.; Raghavachari, K.; Rendell, A.; Burant, J. C.; Iyengar, S. S.; Tomasi, J.; Cossi, M.; Rega, N.; Millam, J. M.; Klene, M.; Knox, J. E.; Cross, J. B.; Bakken, V.; Adamo, C.; Jaramillo, J.; Gomperts, R.; Stratmann, R. E.; Yazyev, O.; Austin, A. J.; Cammi, R.; Pomelli, C.; Ochterski, J. W.; Martin, R. L.; Morokuma, K.; Zakrzewski, V. G.; Voth, G. A.; Salvador, P.; Dannenberg, J. J.; Dapprich, S.; Daniels, A. D.; Farkas, Ö.; Foresman, J. B.; Ortiz, J. V.; Cioslowski, J.; Fox, D. J. *Gaussian 09*, revision B.1; Gaussian, Inc.: Wallingford, CT, 2009.
(27) (a) Schaefer, A.; Horn, H.; Ahlrichs, R. *J. Chem. Phys.* **1992**, *97*, 2571. (b) Schaefer, A.; Huber, C.; Ahlrichs, R. *J. Chem. Phys.* **1994**, *100*, 5829.
(28) (a) Carpenter, J. E.; Weinhold, F. *J. Mol. Struct.* **1988**, *169*, 41. (b) Reed, A. E.; Curtis, L. A.; Weinhold, F. *Chem. Rev.* **1988**, *88*, 899. (c) Weinhold, F.; Carpenter, J. E. *The Structure of Small Molecules and Ions*; Plenum Publishing: New York, 1988; p 227.
(29) (a) Cossi, M.; Rega, N.; Scalmani, G.; Barone, V. *J. Comput. Chem.* **2003**, *24*, 669. (b) Tomasi, J.; Mennucci, B.; Cances, E. *J. Mol. Struct. (THEOCHEM)* **1999**, *464*, 211.